Adaptive Hierarchical Finite Element Modeling of Dopant Diffusion

A. Bose* and C. S. Rafferty**

Bell Laboratories
Lucent Technologies, 700 Mountain Avenue, Murray Hill, NJ 07974
* abose@research.bell-labs.com
** conor@barkeep.div111.bell-labs.com

ABSTRACT

We present a finite element formulation based on a $h-p$ refinement strategy for the coupled dopant-defect diffusion problem in semiconductor process modeling. The algorithm involves increasing the degree p of the element basis as well as mesh refinement (h) and redistribution as an optimal way of generating more accurate approximate solutions to the diffusion problem. A hierarchic family of nested basis functions based on integrated Legendre polynomials is employed in the present study. The lower-degree monomial functions are explicitly embedded in successively higher order bases and therefore, the element matrices and vectors need not be recomputed corresponding to the lower-order bases for each p-refinement. More specifically, an element matrix corresponding to a degree $p = k$ is a nested sub-matrix of the new element matrix corresponding to $p = k + 1$. An important characteristic of the hierarchic monomials is that the coefficients corresponding to the mid-side and interior element nodes are tangential derivatives of the solution field and not necessarily the function values. Numerical examples demonstrate the optimal convergence rate and accuracy of the present formulation.

Keywords: TED, $h-p$ finite element, numerical modeling

INTRODUCTION

The most crucial part of semiconductor process modeling is tracking the movement of dopants introduced into the crystal. The dopant distribution governs every aspect of device behavior. Diffusion of dopants in silicon is mediated by the point defects of the silicon lattice, interstitials and vacancies. The faster dopants diffuse almost exclusively via an interstitial mechanism. As many processing steps in the fabrication of a device locally perturb the concentration of interstitials in the lattice, modeling defect-assisted diffusion is of great importance in modern technology.

The basic equations of defect-mediated diffusion are [1]

$$\frac{\partial B}{\partial t} = \nabla \cdot \mathbf{F}_b \tag{1}$$

$$\frac{\partial I}{\partial t} = \nabla \cdot \mathbf{F}_b + \nabla \cdot \mathbf{F}_i \tag{2}$$

$$\mathbf{F}_b = D_b \left((\frac{I}{I^*}) \nabla B + B \nabla (\frac{I}{I^*}) \right) \tag{3}$$

$$\mathbf{F}_i = D_i I^* \nabla (\frac{I}{I^*}) \tag{4}$$

where B is the concentration of dopants, I is the concentration of free interstitials, I^* is the thermal equilibrium background of interstitials and $\mathbf{F}_b$, $\mathbf{F}_i$ are the local fluxes of defects and interstitials, and D_b is the equilibrium diffusivity of the dopant.

Increases in the interstitial concentration above the background result in two effects; first there is an overall enhancement in the diffusivity of dopants due to the excess interstitials. Secondly, there is an 'uphill' diffusion term which causes dopants to pile up due to gradients of point defects. Such gradients arise near surfaces, where interstitials recombine readily, keeping the surface concentration of defects near equilibrium at all times. Both effects have negative impacts on transistor behavior. The enhanced diffusion washes out carefully tailored dopant profiles and can cause closely separated features to merge. The uphill diffusion can cause undesired piles of dopant to form near surfaces, raising threshold voltage and reducing carrier mobility [2].

When interstitials are generated by ion implantation, the excess above equilibrium is so large that the interstitials coalesce into clusters and maintain a steady enhancement of free interstitials over the background. The relation of free interstitials to total interstitials can be approximated by [3]

$$I = \frac{1}{\left(\frac{1}{I^{tot}} + \frac{1}{sI^*} \right)} = min(I^{tot}, sI^*) \tag{5}$$

where the enhancement s can be several thousand, and I^{tot} is the total local concentration of interstitials.

Note that appropriate boundary and initial conditions must be imposed for a well-posed problem ((1)-(4)). For example, the equations describing diffusion of interstitials can be closed as follows:

$$
\begin{aligned}
I &= g \ on \ \tau_g \times]0.T[\\
-\mathbf{F_i} \cdot \mathbf{n} &= h \ on \ \tau_h \times]0.T[\qquad (6) \\
I(\mathbf{x},0) &= I_0(\mathbf{x}) \qquad (7)
\end{aligned}
$$

The equations for dopant diffusion can also be closed in a similar manner.

GALERKIN FORMULATION

Let $\mathcal{V}^h$ denote the discrete space of weighting functions satisfying the zero boundary conditions on B and I; and $\mathcal{S}^h = \mathcal{S}^h_t$ the discrete space of trial solutions which vary as a function of time. The semi-discrete Galerkin formulation corresponding to the weak form of the interstitial equations can be written as

Given g, h and I_0, find $I^h(t) = v^h + g^h, I^h(t) \in \mathcal{S}^h_t$, $t \in [0,T]$ such that for all $w^h \in \mathcal{V}^h$

$$
\begin{aligned}
(w^h, \dot{v}^h) + a(w^h, v^h) &= (w^h, h)_\tau - (w^h, \dot{g}^h) \qquad (8) \\
(w^h, v^h(\mathbf{x},0)) &= (w^h, I_0) - (w^h, g^h(0)) \qquad (9)
\end{aligned}
$$

The trial solutions v^h and g^h can be written as

$$
\begin{aligned}
v^h &= \sum_{i \in (n - n_g)} \mathcal{N}_i(\mathbf{x})\, v_i(t) \qquad (10) \\
g^h &= \sum_{i \in (n_g)} \mathcal{N}_i(\mathbf{x})\, g_i(t) \qquad (11)
\end{aligned}
$$

where the nodes n_g belong to the boundary segment τ_g.

The corresponding Galerkin weak formulation for the boron equations can be derived in a similar manner. The basis functions $\mathcal{N}_i$ can be constructed using the family of hierarchic polynomials as follows.

Hierarchic basis functions

In the following, we briefly review the hierarchic polynomial shape functions for p-finite element methods and refer to [4] for details.

The basis functions for any element can be organized into vertex, edge and interior functions. These are generated by tensor products of one-parameter family of either Lagrange or Legendre polynomials. Such 1D hierarchic polynomials in parameter $\xi \in [-1,1]$ can be defined as (see Figure 1)

$$
\begin{aligned}
\mathcal{N}_{(1)}(\xi) &= \frac{1}{2}(1-\xi) \\
\mathcal{N}_{(3)}(\xi) &= \frac{1}{2}(1+\xi) \qquad (12) \\
\mathcal{N}^{(i)}{}_{(2)}(\xi) &= \phi_i(\xi)
\end{aligned}
$$

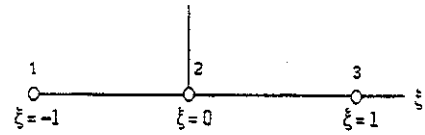

Figure 1: 1D hierarchic basis functions

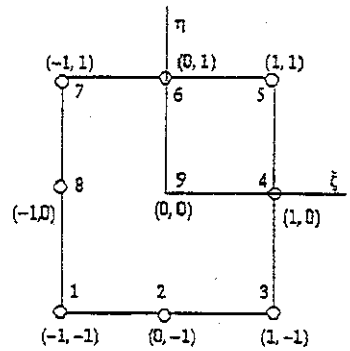

Figure 2: 2D hierarchic basis functions

The functions ϕ_i are polynomials of degree i and can be written for Lagrange polynomials as

$$
\phi_i(\xi) = \left(\xi^i - s\right) \quad i \geq 2 \qquad (13)
$$

where $s = 1$ for i even and $s = \xi$ for i being odd. Similarly, for Legendre polynomials

$$
\phi_i(\xi) = \frac{1}{\sqrt{2(2i-1)}} \left(P_i(\xi) - P_{i-2}(\xi)\right) \qquad (14)
$$

where the polynomials $P_i(\xi)$ are given by the recursive

$$
(n+1)P_{n+1}(\xi) = (2n+1)\xi P_n(\xi) - nP_{n-1}(\xi) \qquad (15)
$$

Generalizing to 2D quadrilaterals, we can identify the basis functions as follows (see Figure 2)

Vertex Basis Functions

$$
\begin{aligned}
\mathcal{N}_1(\xi,\eta) &= \frac{1}{4}(1-\xi)(1-\eta) \\
\mathcal{N}_3(\xi,\eta) &= \frac{1}{4}(1+\xi)(1-\eta) \\
\mathcal{N}_5(\xi,\eta) &= \frac{1}{4}(1+\xi)(1+\eta) \qquad (16) \\
\mathcal{N}_7(\xi,\eta) &= \frac{1}{4}(1-\xi)(1+\eta)
\end{aligned}
$$

(17)

Edge Basis Functions

$$\mathcal{N}_2(\xi,\eta) = \frac{1}{2}\phi_i(\xi)(1-\eta), \quad i = 2.3,\cdots p$$

$$\mathcal{N}_4(\xi,\eta) = \frac{1}{2}(1+\xi)\phi_i(\eta), \quad i = 2.3,\cdots p$$

$$\mathcal{N}_6(\xi,\eta) = \frac{1}{2}\phi_i(\xi)(1+\eta), \quad i = 2,3,\cdots p \qquad (18)$$

$$\mathcal{N}_8(\xi,\eta) = \frac{1}{2}(1-\xi)\phi_i(\eta), \quad i = 2,3,\cdots p$$

(19)

Interior Basis Functions

$$\mathcal{N}_9(\xi,\eta) = \phi_i(\xi)\phi_j(\eta), \quad i,j = 2.3.\cdots p \qquad (20)$$

In the above, the lower-degree monomial functions are explicitly embedded in successively higher order bases and therefore, the element matrices and vectors need not be recomputed corresponding to the lower-order bases for each level of p-refinement. More specifically, an element matrix corresponding to a degree $p = k$ is a nested sub-matrix of the new element matrix corresponding to $p = k + 1$. An important characteristic of these hierarchic monomials is that the coefficients corresponding to the mid-side and interior element nodes are tangential derivatives of the solution field and not necessarily the function values.

In our adaptive p methodology, the polynomial degree may differ on adjacent elements. The polynomial degree p across an element edge is taken to be the smaller p-value of the two adjoining elements sharing that edge. C^0 continuity of field variables across element edges follows easily since the degree can be constrained by simply setting the corresponding higher-order derivatives as degrees of freedom on an edge to zero. However, this need not be done explicitly. For most finite element formulations, this step can be incorporated by assembling only those edge hierarchic basis functions that correspond to polynomial orders less than or equal to p. This results in a smaller linear system of equations to be solved later.

NUMERICAL STUDIES

The main numerical problems in transient enhanced diffusion are that dopant concentrations are significant over a range of four to five decades, the diffusivities of point defects are at least a million times faster than that of the dopants, making the problem stiff; and that drift terms may significantly exceed diffusion terms, often demanding upwinding. A typical problem in this category is modeling the pile up of dopant at the surface induced by the damage distributed at some depth in the crystal.

As a first example, we consider an initially flat boron profile and study the resulting 'pile-up' of boron at the surface due to transient enhanced diffusion. The following initial profiles are imposed:

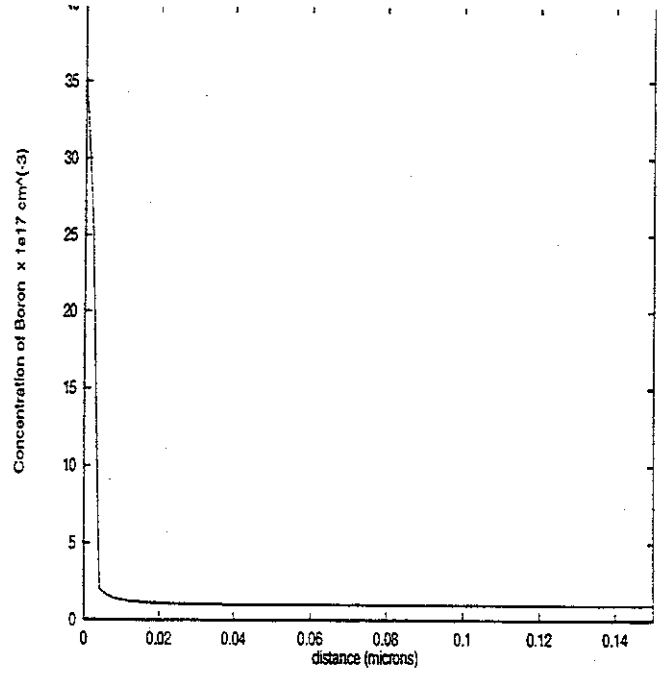

Figure 3: Boron profile at t = 1000s

$$B(x,0) = 10^{17} \ cm^{-3} \qquad (21)$$

$$I(x,0) = 5 \times 10^{13} + 10^{20} e^{-\frac{(x-0.5)^2}{2\times 0.01^2}} \ cm^{-3} \qquad (22)$$

The diffusivities of boron and interstitials are $4 \times 10^{-17}\frac{cm^2}{s}$ and $10^{-8}\frac{cm^2}{s}$ respectively. Figures 3 and 6 show the concentration profiles of boron and defects at $t = 1000$ seconds. The boron concentration at the surface must be computed accurately since it affects the device characteristics. The steep gradients near the surface are usually resolved by using a fine mesh and subsequent mesh refinements. The present approach requires a 'reasonable' initial mesh that does not necessarily resolve the strong boundary layers. The solution is improved by increasing the polynomial degree of the element basis until a converged solution is obtained. Since, an increase in the polynomial degree of an element basis introduces additional unknowns, this step is carried out only in those elements that are close to the surface (the 'pile-up' region).

Figure 4 compares boron concentration values close to the surface ($x = 0$) for different p-refinement levels. A relatively coarse mesh was used for the present study. It is clear that using low order finite elements on this coarse mesh introduces appreciable error in the 'pile-up' value of boron at the surface. However, the correct solution is reached by increasing the element degree to 4 and higher. We compare this approach with

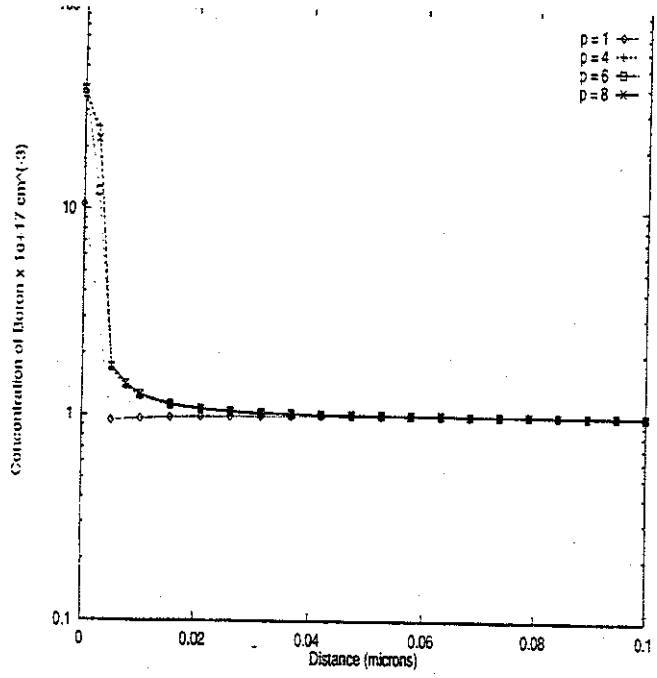

Figure 4: Convergence with increasing polynomial degree

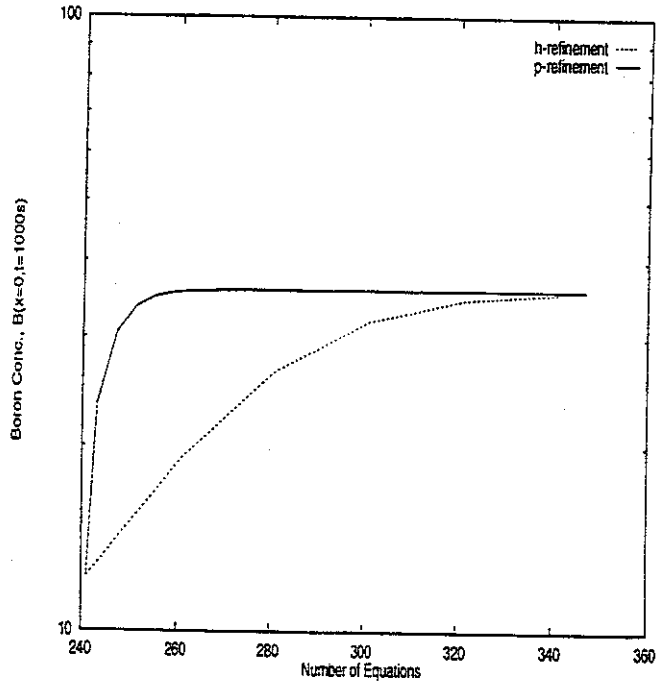

Figure 5: Comparison of h and p-refinement schemes

a conventional h-refinement scheme in Figure 5. Only the elements near the surface are refined successively until convergence. It should be noted that the present p-refinement scheme yields a faster convergence to the surface value of Boron, resulting in a smaller algebraic system to be solved for the discrete problem.

A different set of implanted profiles for boron and point defects are studied next:

$$B(x,0) = 10^{14} + 8 \times 10^{17} e^{-\frac{(x-0.4)^2}{2\times 0.01^2}} + 32 \times 10^{17} e^{-\frac{(x-0.7)^2}{2\times 0.01^2}} \; cm^{-3} \quad (23)$$

$$I(x,0) = 10^{12} + 1.87 \times 10^{19} e^{-\frac{(x-0.5)^2}{2\times 0.01^2}} \; cm^{-3} \quad (24)$$

We show the surface values of boron concentration for different polynomial refinement levels in Figure 7 and compare them with the solution from 'Prophet' simulator for accuracy. As shown earlier, there is significant error in the model for low degree elements. However, the correct profile is obtained by successively increasing the polynomial order of the elements. Note that the mesh used for the present p-refinement study is coarser than the final mesh in 'Prophet' and therefore, results in a smaller number of unknowns. Figures 8 and 9 present the profiles of boron and point defects at various times of the diffusion process and compare the results with those using 'Prophet'.

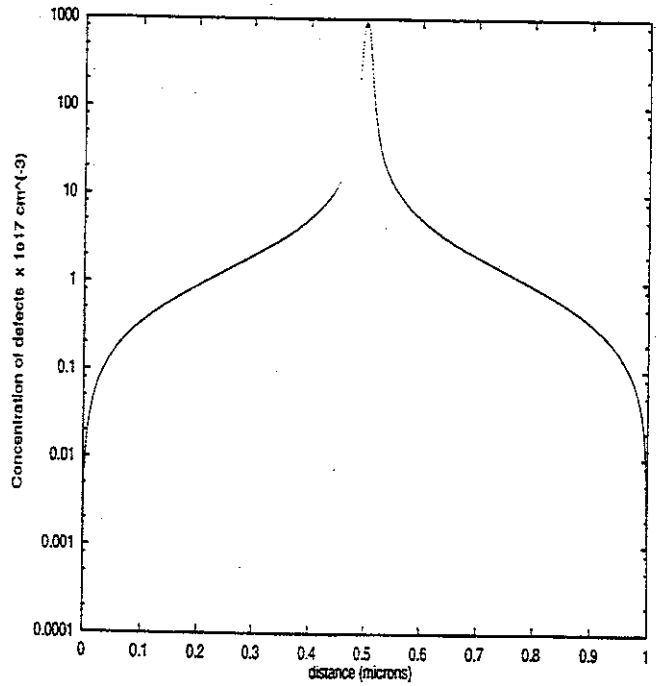

Figure 6: Concentration of defects at t = 1000s

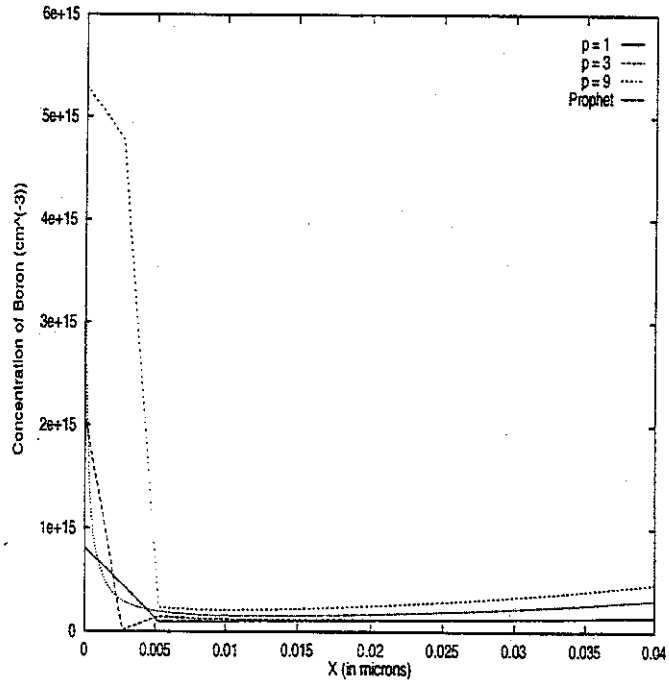

Figure 7: Surface values of Boron at t = 1000s for different p-refinement levels

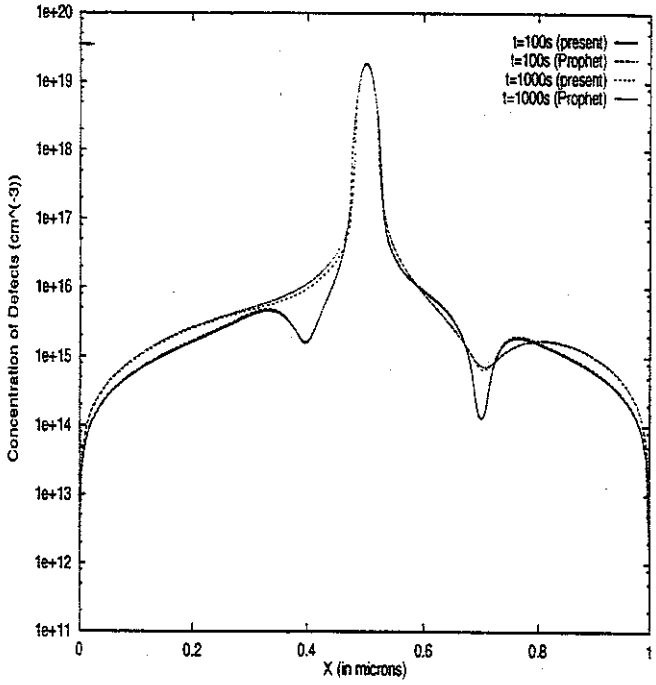

Figure 8: Concentration of point defects at t = 1000s

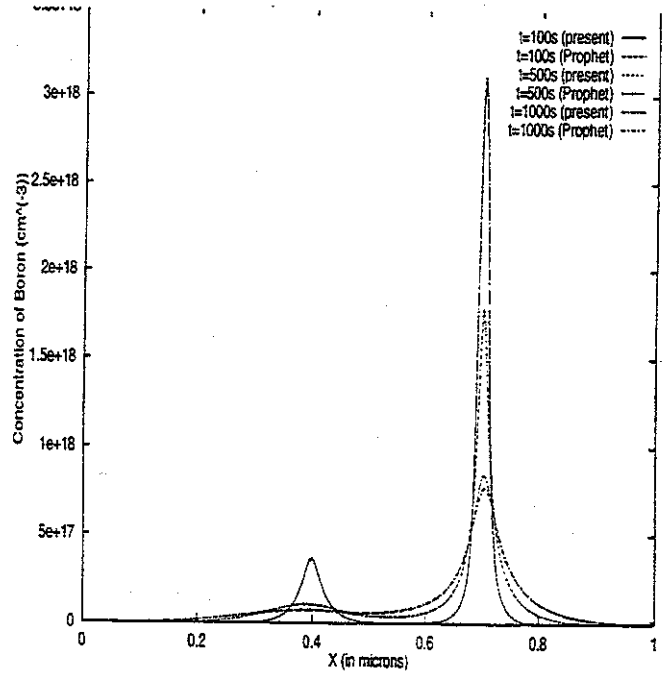

Figure 9: Concentration of Boron at t = 1000s

CONCLUSION

We have presented an adaptive higher-order finite element formulation for modeling transient enhanced diffusion in semiconductor process modeling. We advise a combination of mesh refinement and polynomial enrichment of the element basis functions for problems with steep gradients and strong singularities to effectively contain the pollution error. Nevertheless, in the pre-asymptotic range, selective p-refinement is often very effective. This should not be ignored since in many engineering applications, accuracy requirements do not warrant computations in the asymptotic range. The numerical examples presented above confirm the higher rate of convergence with the p-refinement method as compared to linear finite element schemes commonly used in process simulation codes.

REFERENCES

[1] P.B. Fahey, P.B. Griffin, J.D. Plummer, Reviews of Modern Physics, 61(2), 289, 1989.

[2] C.S. Rafferty, H.-H. Vuong, S.A. Eshraghi, M.D. Giles, M.R. Pinto, S.J. Hillenius, Proceedings of the 1993 International Electron Device Meeting, Washington, 311, Dec 1993.

[3] C.S. Rafferty, G.H. Gilmer, M. Jaraiz, D. Eaglesham, H-J. Gossmann, Applied Physics Letters, 68(17) 2395, 1996.

[4] B. Szabo, I. Babuska, "Finite Element Analysis", John Wiley and Sons, Inc., 1991.